

## Physicochemical Characterization and Controlled Release Formulation on Intercalated 2-Methyl-4-chlorophenoxy Acetic Acid-Graphite Oxide (MCPA-GO) Nanocomposite

Norilyani Izzati Hasanuddin<sup>1</sup>, Nur Nadia Dzulkifli<sup>1</sup>, Siti Halimah Sarijo<sup>2</sup>, and Sheikh Ahmad Izaddin Sheikh Mohd Ghazali<sup>1,\*</sup>

<sup>1</sup>Faculty of Applied Sciences, Universiti Teknologi MARA, Campus Kuala Pilah, 72000, Kuala Pilah, Negeri Sembilan, Malaysia

<sup>2</sup>Faculty of Applied Sciences, Universiti Teknologi MARA Shah Alam, 40450, Shah Alam, Selangor, Malaysia

\* Corresponding author:

email:

sheikhahmadizaddin@ns.uitm.edu.my

Received: August 3, 2018

Accepted: December 11, 2018

DOI: 10.22146/ijc.40921

**Abstract:** In this present work, herbicide named 2-methyl-4-chlorophenoxy acetic acid (MCPA) was intercalated into the graphite oxide through ion-exchange method to produce an MCPA-GO nanocomposite as an herbicide delivery system. The formation of MCPA-GO nanocomposite was confirmed by using PXRD, Fourier Transform Infrared Spectroscopy (FTIR), Thermal Gravimetric Analysis (TGA), UV-Visible Spectroscopy and Accelerated Surface Area Surface (ASAP). As for PXRD pattern, there was increasing in the basal spacing of the nanocomposite from the graphite oxide which by 9.3 to 9.7 Å indicated that MCPA has successfully inserted into the interlayers of the graphite oxide. Meanwhile, the FTIR spectrum showed the appearance of a new peak in MCPA-GO nanocomposite at 1308 cm<sup>-1</sup> represents the functional group of carboxylate (COO<sup>-</sup>). This peak is very necessary for the confirmation of the anionic form of MCPA inserted into the interlayers of graphite oxide. The controlled release property was also done for further investigation by using various aqueous media to determine the percentage release of MCPA from the nanocomposite. The percentage of herbicide release in Na<sub>3</sub>PO<sub>3</sub> solution was higher than in Na<sub>2</sub>CO<sub>3</sub> and NaCl solution proved that the release properties exhibit the potential application of graphite oxide as effective nanocarrier of herbicides. MCPA-GO nanocomposite suggested being most promising herbicide since it can lower the toxicity of precursor MCPA, high biocompatibility, and more efficient in herbicide delivery system.

**Keywords:** 2-methyl-4-chlorophenoxy acetic acid; graphite oxide; herbicide; nanocomposite

### ■ INTRODUCTION

Agricultural growth has been a strong pathway to define the economy of agro-based countries. In Malaysia alone, 12% of National Gross Domestic Product are emanated from the agricultural industry itself that providing about 16% of employment of current population. Correspondingly, the agricultural economists and chemists tend to focus on how to robust the agricultural growth as well as productivity and give a little attention to the side effect of agrochemical usage. As a result, pesticides, herbicides, and plant growth regulator have been widely used in modern agriculture. According

to the Environmental Protection Agency (EPA) in the United States, 2-methyl-4-chlorophenoxy acetic acid (MCPA) is an example of herbicide that was sold approximately 4.6 million pounds each year for agricultural and residential usage. MCPA is a specific systemic chemical herbicide that applied to kill or inhibit the growth of specific plants such as noxious weed plant in cereals, wheat, rice, corn, peas, potatoes and grasslands [1]. However, the environmental problems arise once the residue of herbicide being swept away by rain that leads to soil pollution, strong water pollutant and they difficult to degrade and can rapidly move

around [2-3]. Besides, human health may also be affected by drinking water and direct exposure. Touloupakis et al. [4] mentioned in their journal that direct exposure of MCPA can worsen the health from asthma and skin rashes to chronic disorders.

The persistent of this slightly hazardous agrochemical, if accumulated in the environment, will increase the risks to human health. Many studies on the adsorption of pesticides by clay minerals for their removal from water and its immobilization in soils can be found in the open literature; however, studies on the increase the efficiency of the agrochemicals and reducing their leaching into the environment are very limited. A few attempts were made to intercalate the herbicide with a clay mineral, layered double hydroxide (LDH) and many other ways. However, there is no study reported yet by using graphite oxide as a nanocarrier. Contrarily, the percentage loading of drug/herbicides of the graphite oxide could reach up to 200% [11] which is considerably higher compared with other drugs/herbicides delivery systems or nanocomposite that usually have a loading percentage lower than 100%. It has been suggested that intercalation of herbicide with graphite oxide would be one of the feasible solutions.

Graphite oxide has been explored enormously as an exciting topic by the researchers in various fields such as electronic [5], catalysis, biosensors [6] and biomedical application [7]. In the current area of biomedical, the intercalation of the graphite oxide (GO) had received tremendous attention solely to emerge as new and competitive drugs delivery systems with the potential of targeting nanocarrier or host. It is because they are facilitating the good targeting, high loading and control release of drugs/herbicides. By exploring the area drugs delivery system, Barahuie et al. [8] have reported the graphite oxide as a nanocarrier for the active anticancer agent of chlorogenic acid while Dorniani et al. [9], makes their research on gallic acid as a cancer therapy by using the graphite oxide too. Besides that, Yu et al. [10] did some modification in their work to make the graphite oxide being able to be as a nanocarrier loaded with anticancer herbal drug berberine by combined the graphite oxide with PEG.

To the best of our knowledge, there is no literature reported yet in the field of herbicides delivery system by using graphite oxide as a nanocarrier. Therefore, in this present work, MCPA was intercalated into the graphite oxide to produce a better and even the safer improvise herbicide that may minimize the environmental problems and yet, still provide the maximum outcomes to the desirable plants. In addition, the residue or excess herbicide can be lessened by controlled-release (CR) formulations that make the herbicide exist in the interlayer region of graphite oxide and allows the herbicide to be released dependent to the desired concentration over the time. Moreover, it is green chemistry that would also consider environmental safety. This herbicide is environmentally friendly since it can naturally reduce in the environment through the action of ubiquitous *Shewanella* bacteria or decomposes to humic acids [11-12].

## ■ EXPERIMENTAL SECTION

### Materials

Graphite powder and MCPA were purchased from Sigma Aldrich and were used without further purification. Sulphuric acid (98%), potassium permanganate, hydrochloric acid (35%), hydrogen peroxide and ethanol (98%), were obtained from R & M Chemical. All the solutions were prepared by using deionized water.

### Procedure

#### **Synthesis of graphite to graphite oxide**

Graphite oxide was prepared by using the improved Hummer's Method. One gram of graphite powder and 23 mL of concentrated sulphuric acid were mixed in a beaker under mechanical stirring (150 rpm). The ice bath was placed under the beaker. Then, 3.0 g of potassium permanganate ( $\text{KMnO}_4$ ) was added slowly into the beaker to keep the temperature of the suspension lower than 20 °C. Next, the reaction system was transferred to a 40 °C of oil bath for 30 min. In the beaker, 50 mL of deionized water was poured and the solution was stirred for 15 min at 95 °C. After that, 150 mL of deionized water was added and followed by a dropwise addition of 5 mL of 30% hydrogen peroxide.

During this step, the color of the solution was turned from dark brown to yellow color. The mixture was filtered and washed them with the hydrochloric acid aqueous solution to remove metal ions. Lastly, the precipitate was dried at 60 °C in the vacuum oven for 48 h.

### Synthesis of MCPA-GO nanocomposite

The MCPA-GO nanocomposite was done by using ion-exchanged method [1]. This method was run under the room temperature. First, about 0.35 g of the prepared graphite oxide was reacted with 25 mL aqueous solution of MCPA in the 100 mL volumetric flask. As the mixture of graphite oxide and MCPA was mixed together, the mixture was stirred for 5 h on the hotplate before aging for 18 h at 70 °C in an oil bath shaker. Then, the slurry solution was taken for centrifuged at 180 rpm in 5 min and washed several times with deionized water. The product obtained was dried in an oven at a temperature of 70 °C for 72 h. The sample then is kept in a sample bottle for further characterization by using PXRD, FTIR and CHNS analysis.

### Controlled release study of MCPA-GO nanocomposite

The release of MCPA from MCPA-GO nanocomposite was prepared with different aqueous media which were sodium phosphate ( $\text{Na}_3\text{PO}_4$ ), sodium carbonate ( $\text{Na}_2\text{CO}_3$ ) and sodium chloride ( $\text{NaCl}$ ). Three milligrams of MCPA-GO nanocomposite was placed in the quartz cuvette on top of aqueous media. The percentage release of MCPA from MCPA-GO nanocomposite was measured by using a UV-Vis instrument with a wavelength of 237 nm.

## RESULTS AND DISCUSSION

### PXRD Analysis

Fig. 1 shows the XRD patterns for the graphite, graphite oxide and MCPA-GO nanocomposite. The basal spacing of these samples was calculated by using Bragg's Law as shown in Eq. (1).

$$n\lambda = 2d\sin\theta \quad (1)$$

As for graphite, the strong and sharp diffraction peak located in (003) orientation was observed at  $2\theta = 26.5^\circ$  corresponding to the basal spacing of 3.4 Å. The PXRD pattern revealed that graphite has high crystallinity

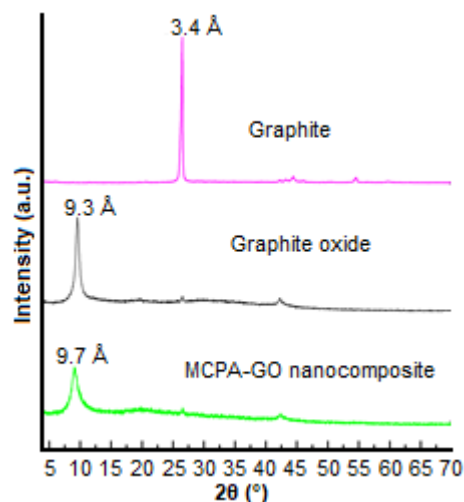


Fig 1. XRD pattern for graphite, GO and MCPA-GO nanocomposite

due to highly organized delocalized  $\pi$  hexagonal rings structure with  $120^\circ$  angle between each carbon atom in the plane of the layers [13]. Other than that, GO showed an intense and very strong peak at  $2\theta = 9.54^\circ$  with diffraction orientation of (002). The increment of basal spacing around 9.3 Å of GO signifies the functionalization of the graphite was successful with the formation of oxygen-functional groups such as hydroxyl group, epoxide, and carboxyl group as well as water molecules at the edge and basal planes of sheets after the harsh chemical oxidation process [14-15].

The peak was shifted downwards to  $2\theta = 9.10^\circ$  and became wider with a basal spacing of 9.7 Å after the intercalation process took place. The expansion of the interlayers of the nanocomposite with only single peak present has confirmed the inclusion of herbicide anion, MCPA during intercalation process. This extent of expansion may be due to several factors such as the anionic size of herbicide, charge, orientation, and interaction between graphite oxide and herbicide [1]. Theoretically, the intercalation of MCPA with graphite oxide involved non-covalent dynamic bonding interactions such as hydrogen bonding,  $\pi$ - $\pi$  stacking, and electrostatic forces bounding to each other due to the presence of oxygen groups as the reactive sites [16]. The nanocomposite was analyzed with other complimentary analysis for further confirmation.

### FTIR Spectra

Fig. 2 shows the FTIR-ATR spectra for GO, MCPA and MCPA-GO nanocomposite. In the GO spectrum, O-H stretching vibrations peak was found at  $3362\text{ cm}^{-1}$  that corresponds to the carboxyl and hydroxyl groups and residual water in interlayers of GO. These functional groups enable GO to have better dispersibility in water [16]. Besides that, C=C bonds were detected at  $1626\text{ cm}^{-1}$  indicating the main structure of graphite remained and unoxidized. A peak at  $1730\text{ cm}^{-1}$  was referred to the stretching vibration of the C=O bond demonstrating the presence of carboxylic acid. Other vital peaks at  $1221$  and  $1050\text{ cm}^{-1}$  were represented the functional group of epoxy (C-O) and alkoxy group (C-O), respectively. These oxygenated functional groups indeed confirmed the graphite had oxidized into GO which consistent with the literature [16-17].

For MCPA, peak at  $2910\text{ cm}^{-1}$  represented the hydroxyl group (O-H) from the vibration of the COOH [18], and another peak at  $2878\text{ cm}^{-1}$  signify the substituent of the methyl group. Next, the functional group of C=O stretching was detected at the sharp peak of  $1707\text{ cm}^{-1}$ .

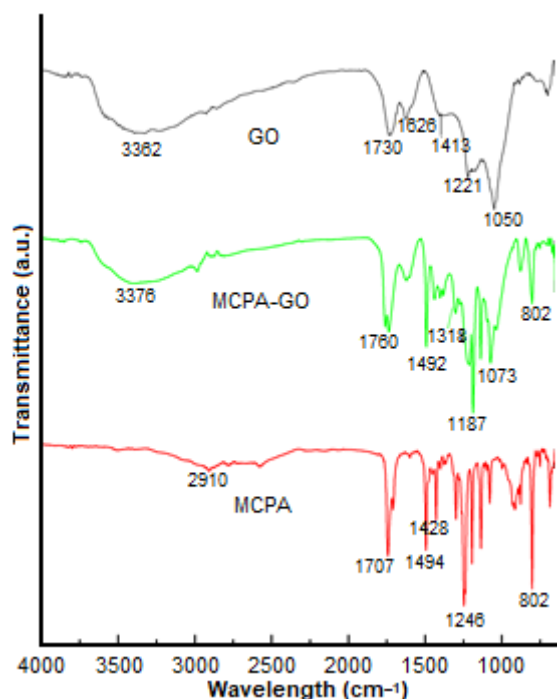


**Fig 2.** FTIR-ATR spectra for GO, MCPA and MCPA-GO nanocomposite

The peaks at  $1494$  and  $1428\text{ cm}^{-1}$  were corresponding to the C=C, and a strong peak at  $1298\text{ cm}^{-1}$  assemble the symmetric and asymmetric stretching mode of C-O-C vibration. A sharp peak at  $802\text{ cm}^{-1}$  has been observed that belongs to the peak of C-Cl stretching.

The FTIR spectrum of MCPA-GO nanocomposite have exhibited the peaks resembles MCPA and graphite oxide spectra. The characteristic peaks of  $1760\text{ cm}^{-1}$  with high intensity attributed to the stretching vibration of carbonyl groups of carboxylic group present. An observation of a new peak at  $1308\text{ cm}^{-1}$  primarily due to the C=O vibration of the carboxylate anion as the result of intercalation. Furthermore, an obvious broad absorption peak at  $3377\text{ cm}^{-1}$  was assigned to the O-H stretching vibration due to water molecules present in the nanocomposite.

### UV-Vis Spectrum

Fig. 3 shows the UV-Visible spectrums for GO, MCPA and MCPA-GO nanocomposite. The spectra were analyzed by using range between  $200\text{ nm}$  until  $400\text{ nm}$ . The vital transitions for GO were ( $n \rightarrow \sigma^*$ ) and ( $\pi \rightarrow \pi^*$ ). The absorption was observed at  $245\text{ nm}$  due to the aromatic C=C bond for transition ( $n \rightarrow \sigma^*$ ) [19]. Furthermore, the absorption peak at  $300\text{ nm}$  was stood for C=O bond transition ( $\pi \rightarrow \pi^*$ ). For transition ( $n \rightarrow \sigma^*$ ) in MCPA, the wavelength at  $230\text{ nm}$  was recorded in

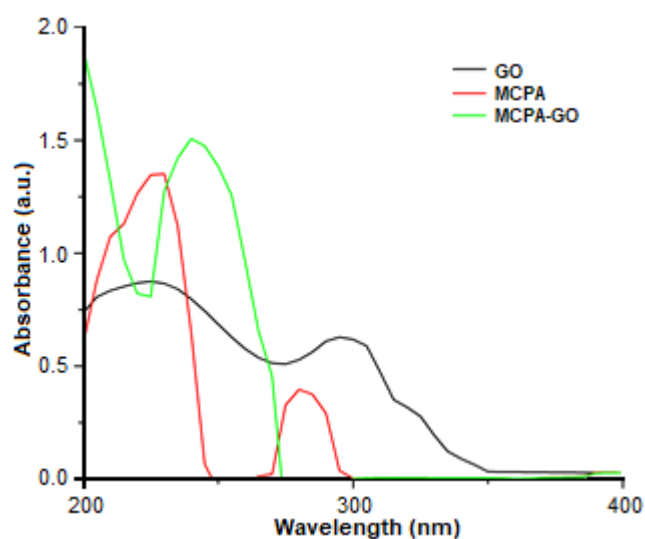


**Fig 3.** UV-Visible spectrums for GO, MCPA and MCPA-GO nanocomposite

which contributed to a carbonyl group where the excitation of the electron occurred in an unshared pair on oxygen to antibonding  $\sigma$  orbital. At 280 nm, ( $\pi \rightarrow \pi^*$ ) transition presence due to the existence of carboxyl group. In contrast for MCPA-GO nanocomposite, ( $n \rightarrow \sigma^*$ ) and ( $\pi \rightarrow \pi^*$ ) transitions were shifted to lower wavelength with higher absorbance after intercalation between MCPA and GO occurred. This shifting was known as hypsochromic shift primarily due to withdrawing of oxygen electron from carbonyl carbon. But, ( $n \rightarrow \pi^*$ ) was absent in this spectra may due to weak transition due to Laporte Forbidden and high probably the transition was overlapped with ( $n \rightarrow \sigma^*$ ).

### Thermal Analysis

TGA/DTG graphs of GO, MCPA, and MCPA-GO nanocomposite were displayed in Fig. 4. This is another complimentary techniques used for the confirmation of MCPA nanocomposite. Based on Fig. 4(a), GO showed

two major stages of thermal decomposition in the region of 125–150 °C and 210–243 °C. The first stage occurred at the maximum temperature of 141 °C with a weight loss of 14% that associated with the removal of water molecules between the interlayers of GO. It was followed by the second stage with a sharp peak at 226 °C. This decomposition mainly due to the loss of unstable oxygenated functional groups with 24% weight loss. Next, Fig. 4(b) exhibited the decomposition of MCPA that corresponding to an intense peak at 217 °C. The weight loss occurred was 98.6% that primarily due to the decomposition and combustion organic matter of MCPA.

As expected, two stages of weight loss were observed through the TGA/DTG analysis of MCPA-GO nanocomposite in Fig. 4(c). Firstly, a rough 7% of weight loss occurred at a temperature of 123 °C which owing to the elimination of water molecules present. The second major stage was detected at 486 °C with the weight loss

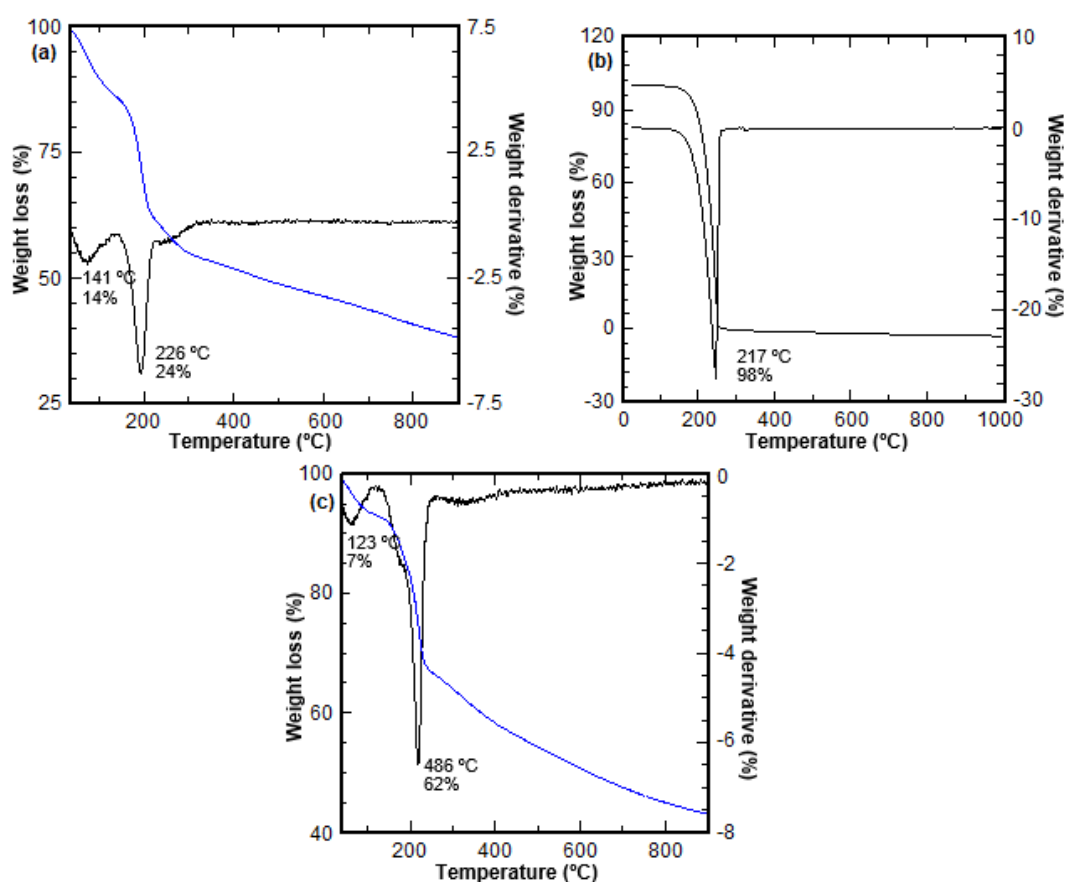


Fig. 4. TGA/DTG thermogram of (a) GO, (b) MCPA and (c) MCPA-GO nanocomposite

of 32%. This stage was attributed to the decomposition of oxygenated functional groups and organic anion, MCPA that present in the MCPA-GO nanocomposite. From the results above, MCPA-GO nanocomposite indeed has higher thermal stability than pristine GO and MCPA.

### Surface Properties

The surface area of GO and MCPA-GO nanocomposite were investigated to verify the successful intercalation process. The intercalation took place with the increased surface area of nanocomposite which was  $8.4887 \text{ m}^2/\text{g}$  whereas the surface area of GO was only  $3.5274 \text{ m}^2/\text{g}$ . The enlargement d-spacing due to the intercalation of a bigger anion, i.e., MCPA, in nanocomposite and will generate more pores in the crystallites. Thus, the surface area of nanocomposite increase significantly. Through the adsorption-desorption isotherms in Fig. 5, GO was identified to have microporous-type of material while MCPA-GO nanocomposite had an open loop in its graph. The BJH desorption pore size

distribution for GO and MCPA-GO nanocomposite was observed in Fig. 6. From the results obtained, MCPA-GO nanocomposite had higher pore size distribution centered at  $1938 \text{ \AA}$  than GO. This is related to the involvement of different size of the anion, interstitial pores between the crystallite and accumulation process during the formation of the nanocomposite.

### Controlled Release Studies

The release profile for the controlled release study of MCPA in various aqueous solution was displayed in Fig. 7. The release of MCPA anion from MCPA-GO nanocomposite was recognized due to the  $\pi$ - $\pi$  stacking interaction and hydrophobic bonding between MCPA and graphite oxide [20-21]. Besides, charge-density of the anion of aqueous media solution will also contribute to this phenomenon. Based on Fig. 7, the amount release of MCPA was found to be higher in  $\text{Na}_3\text{PO}_3 > \text{Na}_2\text{CO}_3 > \text{NaCl}$  depending on the availability of an anion in the aqueous solutions.

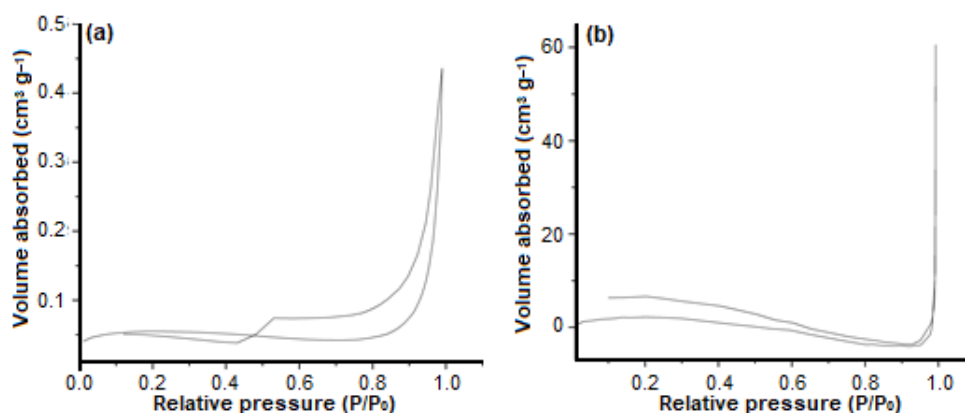


Fig 5. Adsorption-desorption isotherms of (a) GO and (b) MCPA-GO nanocomposite

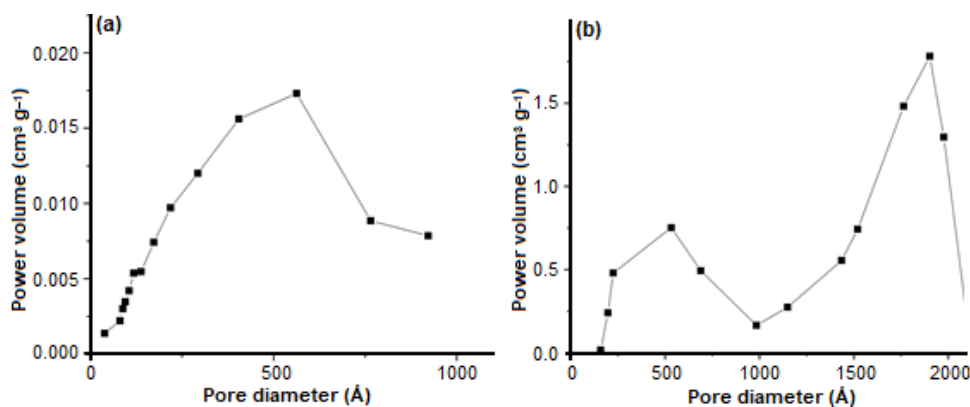
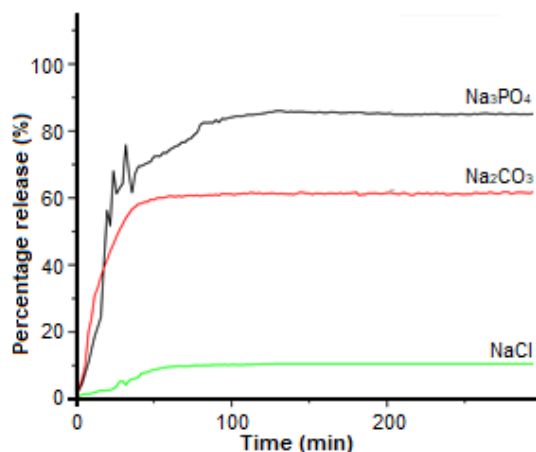


Fig 6. BJH pore size distribution of (a) GO and (b) MCPA-GO nanocomposite



**Fig 7.** The controlled release of MCPA in  $\text{Na}_3\text{PO}_4$ ,  $\text{Na}_2\text{CO}_3$  and  $\text{NaCl}$  solution

The percentage release of MCPA was found to be 85, 61, and 10% in  $\text{Na}_3\text{PO}_3$  solution,  $\text{Na}_2\text{CO}_3$  solution and  $\text{NaCl}$  solution at the time of 116, 60, and 128 min, respectively. It is because  $\text{PO}_3^{3-}$  has a higher charge density than  $\text{CO}_3^{2-}$  and  $\text{Cl}^-$  causes more phosphite ion to be ion-exchanged with MCPA [1]. Phosphite ion that has high affinity towards graphite oxide interlayers enable the phosphite ion from aqueous media to exchange with the intercalated herbicide anion [22]. As a result, phosphite ion is incorporated into the interlayer of graphite oxide and at the same time, the MCPA will be released into the aqueous solutions.

Additionally, the burst effect that presence in the graph of the  $\text{Na}_3\text{PO}_3$  solution may occur due to the surface characteristics of a graphite oxide material, the herbicide interactions and porous structure of the material [9]. The characteristics of the mechanism of the ion-exchange method would not lead the percentage of MCPA anion released from MCPA-GO nanocomposite at equilibrium reach 100%. This is because even though the anion was removed continuously but the loaded anions cannot be exchanged completely at equilibrium. These results show that the MCPA-GO nanocomposite has good potential to be used as an herbicide delivery system with sustainable controlled release properties.

## ■ CONCLUSION

We had successfully developed herbicide delivery system by using graphite oxide as a nanocarrier for MCPA

with sustainable controlled release property. The successful formation of the nanocomposite was characterized by using PXRD, FTIR, TGA, UV-Visible Spectroscopy and ASAP. The FTIR spectrum of this nanocomposite was showed the resemblance of spectrum MCPA and graphite oxide while the appearance of only one strong peak with the wider basal spacing of 9.7 Å in XRD pattern proved that MCPA was successfully intercalated into the graphite oxide. In addition, the controlled release studies were done to figure out the percentage release of the MCPA in various aqueous media. As a result, GO revealed a sustainable of controlled release properties that made GO as a most promising nanocarrier. MCPA-GO nanocomposite has demonstrated the better properties of MCPA by lowering its toxicity, hence increasing the efficiency of its herbicide delivery system.

## ■ ACKNOWLEDGMENTS

This research was funded by the Ministry of Higher Education (MOHE) under the FRGS grant no. 600IRMI/FRGS5/3(66/216). The authors also would like to thank the Department of Academic Affairs of Universiti Teknologi Mara (UiTM) Negeri Sembilan Branch Kuala Pilah Campus for providing the fund and the facilities to carry out this study.

## ■ REFERENCES

- [1] Sarijo, S.H., Ghazali, S.A.I.S.M., and Hussein, M.Z., 2015, Synthesis of dual herbicides-intercalated hydrotalcite-like nanohybrid compound with simultaneously controlled release property, *J. Porous Mater.*, 22 (2), 473–480.
- [2] Al-Zaben, M.I., and Mekhamer, W.K., 2017, Removal of 4-chloro-2-methyl phenoxy acetic acid pesticide using coffee wastes from aqueous solution, *Arabian J. Chem.*, 10 (Suppl. 2), S1523–S1529.
- [3] Touloupakis, E., Margelou, A., and Ghanotakis, D.F., 2011, Intercalation of the herbicide atrazine in layered double hydroxides for controlled-release applications, *Pest Manage. Sci.*, 67 (7), 837–841.
- [4] Nejati, K., Davari, S., Rezvani, Z., and Dadashzadeh, M., 2015, Adsorption of 4-chloro-2-methylphenoxy

- acetic acid (MCPA) from aqueous solution onto Cu-Fe-NO<sub>3</sub> layered double hydroxide nanoparticles, *J. Chin. Chem. Soc.*, 62 (4), 371–379.
- [5] Jeong, H.K., Lee, Y.P., Jin, M.H., Kim, E.S., Bae, J.J., and Lee, Y.H., 2009, Thermal stability of graphite oxide, *Chem. Phys. Lett.*, 470 (4-6), 255–258.
- [6] Kumar, A., and Lee, C.H., 2013, “Synthesis and Biomedical Applications of Graphene: Present and Future Trends”, in *Advances in Graphene Science*, Eds., Aliofkhaezrai, M., IntechOpen, 55–75.
- [7] Wang, Y., Li, Z., Wang, J., Li, J., and Lin, Y., 2011, Graphene and graphene oxide: Biofunctionalization and applications in biotechnology, *Trends Biotechnol.*, 29 (5), 205–212.
- [8] Barahuie, F., Hussein, M.Z., Fakurazi, S., and Zainal, Z., 2014, Development of drug delivery systems based on layered hydroxides for nanomedicine, *Int. J. Mol. Sci.*, 15 (5), 7750–7786.
- [9] Dorniani, D., Saifullah, B., Barahuie, F., Arulsevan, P., Hussein, M.Z.B., Fakurazi, S., and Twyman, L.J., 2016, Graphene oxide-gallic acid nanodelivery system for cancer therapy, *Nanoscale Res. Lett.*, 11, 491.
- [10] Yu, D., Ruan, P., Meng, Z., and Zhou, J., 2015, The Structure-dependent electric release and enhanced oxidation of drug in graphene oxide-based nanocarrier loaded with anticancer herbal drug berberine, *J. Pharm. Sci.*, 104 (8), 2489–2500.
- [11] Zhang, L., Xia, J., Zhao, Q., Liu, L., and Zhang, Z., 2010, Functional graphene oxide as a nanocarrier for controlled loading and targeted delivery of mixed anticancer drugs, *Small*, 6 (4), 537–544.
- [12] Ceriotti, G., Romanchuk, A.Y., Slesarev, A.S., and Kalmykov, S.N., 2015, Rapid method for the purification of graphene oxide, *RSC Adv.*, 5 (62), 50365–50371.
- [13] Chowdhury, D.R., Singh, C., and Paul, A., 2014, Role of graphite precursor and sodium nitrate in graphite oxide synthesis, *RSC Adv.*, 4 (29), 15138–15145.
- [14] Dreyer, D.R., Park, S., Bielawski, C.W., and Ruoff, R.S., 2010, The chemistry of graphene oxide, *Chem. Soc. Rev.*, 39 (1), 228–240.
- [15] Song, J., Wang, X., and Chang, C.T., 2014, Preparation and characterization of graphene oxide, *J. Nanomater.*, 2014, 276143.
- [16] Bardajee, G.R., Hooshyar, Z., Farsi, M., Mobini, A., and Sang, G., 2017, Synthesis of a novel thermo/pH sensitive nanogel based on salep modified graphene oxide for drug release, *Mater. Sci. Eng., C*, 72, 558–565.
- [17] Chen, J., Li, Y., Huang, L., Li, C., and Shi, G., 2014, High-yield preparation of graphene oxide from small graphite flakes via an improved Hummers method with a simple purification process, *Carbon*, 81, 826–834.
- [18] Marcano, D.C., Kosynkin, D.V., Berlin, J.M., Sinitskii, A., Sun, Z., Slesarev, A., Alemany, L.B., Lu, W., and Tour, J.M., 2010, Improved synthesis of graphene oxide, *ACS Nano*, 4 (8), 4806–4814.
- [19] Salleh, N.M., Mohsin, S.M.N., Sarijo, S.H., and Ghazali, S.A.I.S.M., 2017, Synthesis and physico-chemical properties of zinc layered hydroxide-4-chloro-2-methylphenoxy acetic acid (ZMCPA) nanocomposite, *IOP Conf. Ser. Mater. Sci. Eng.*, 204, 012012.
- [20] Han, W., Niu, W.Y., Sun, B., Shi, G.C., and Cui, X.Q., 2016, Biofabrication of polyphenols stabilized reduced graphene oxide and its anti-tuberculosis activity, *J. Photochem. Photobiol., B*, 165, 305–309.
- [21] Liu, H., Li, T., Liu, Y., Qin, G., Wang, X., and Chen, T., 2016, Glucose-reduced graphene oxide with excellent biocompatibility and photothermal efficiency as well as drug loading, *Nanoscale Res. Lett.*, 11 (1), 211.
- [22] Lv, Y., Tao, L., Bligh, S.W.A., Yang, H., Pan, Q., and Zhu, L., 2016, Targeted delivery and controlled release of doxorubicin into cancer cells using a multifunctional graphene oxide, *Mater. Sci. Eng., C*, 59, 652–660.
- [23] Sarijo, S.H., Hussein, M.Z., Yahaya, A.H.J., and Zainal, Z., 2010, Effect of incoming and outgoing exchangeable anions on the release kinetics of phenoxy herbicides nanohybrids, *J. Hazard. Mater.*, 182 (1-3), 563–569.